Cerebral Cortex December 2010;20:2852–2862
doi:10.1093/cercor/bhq035
Advance Access publication March 17, 2010

Longitudinal Analysis of Neural Network Development in Preterm Infants

Christopher D. Smyser[1,2], Terrie E. Inder[1,2,3], Joshua S. Shimony[3], Jason E. Hill[4], Andrew J. Degnan[3], Abraham Z. Snyder[1,3] and Jeffrey J. Neil[1,2,3]

[1]Department of Neurology, [2]Department of Pediatrics, [3]Mallinckrodt Institute of Radiology and [4]Division of Biology and Biomedical Sciences, Washington University School of Medicine, Saint Louis, MO 63110-1093, USA

Address correspondence to Christopher D. Smyser, Department of Neurology, Division of Pediatric Neurology, Washington University School of Medicine, 660 South Euclid Avenue, Campus Box 8111, Saint Louis, MO 63110-1093, USA. Email: smyserc@neuro.wustl.edu.

Application of resting state functional connectivity magnetic resonance imaging (fcMRI) to the study of prematurely born infants enables assessment of the earliest forms of cerebral connectivity and characterization of its early development in the human brain. We obtained 90 longitudinal fcMRI data sets from a cohort of preterm infants aged from 26 weeks postmenstrual age (PMA) through term equivalent age at PMA-specific time points. Utilizing seed-based correlation analysis, we identified resting state networks involving varied cortical regions, the thalamus, and cerebellum. Identified networks demonstrated a regionally variable age-specific pattern of development, with more mature forms consisting of localized interhemispheric connections between homotopic counterparts. Anatomical distance was found to play a critical role in the rate of connection development. Prominent differences were noted between networks identified in term control versus premature infants at term equivalent, including in the thalamocortical connections critical for neurodevelopment. Putative precursors of the default mode network were detected in term control infants but were not identified in preterm infants, including those at term equivalent. Identified patterns of network maturation reflect the intricate relationship of structural and functional processes present throughout this important developmental period and are consistent with prior investigations of neurodevelopment in this population.

Keywords: developmental neuroimaging, functional connectivity MRI, neural networks, preterm infant, thalamocortical connectivity

Introduction

The creation of neural networks is central to cortical development as it has been shown that neural activity—both endogenous and sensory driven—is critical for refining and shaping the intricate circuitry of the nervous system (Penn and Shatz 1999). Many of these networks are initially established during the second half of gestation and involve both corticocortical and thalamocortical connections (Kostovic and Jovanov-Milosevic 2006). Resting state functional connectivity magnetic resonance imaging (fcMRI), applied to prematurely born human infants, offers a noninvasive means by which to monitor the establishment and maturation of these networks in the developing human brain.

fcMRI utilizes temporal correlations in low-frequency (<0.1 Hz) spontaneous fluctuations in blood oxygen level–dependent (BOLD) signal to identify networks with synchronous neuronal activity (Biswal et al. 1995; Lowe et al. 1998; Beckmann et al. 2005; Fox et al. 2005; Damoiseaux et al. 2006). Application of this method in adults has led to the identification of networks encompassing regions of the brain involved in language, attention, behavior, sensation, motor function, visual and auditory stimulus processing, and the default mode (Biswal et al. 1995; Raichle et al. 2001; Fox et al. 2005; Damoiseaux et al. 2006; Dosenbach et al. 2007; Fox and Raichle 2007). Due to the limited demands for subject participation (the subject is studied while resting quietly) and the ease of consistent longitudinal study, fcMRI represents an ideal technique for the study of cerebral development in infants and children. Recent investigations have established the utility of fcMRI in the study of neurodevelopment (Fair, Dosenbach, et al. 2007; Fransson et al. 2007, 2009; Fair et al. 2008; Lin et al. 2008; Liu et al. 2008; Thomason et al. 2008; Kelly et al. 2009). These studies have demonstrated that children possess immature forms of many of the networks described in adults (Fair, Dosenbach, et al. 2007; Fair et al. 2008; Thomason et al. 2008; Fransson et al. 2009; Kelly et al. 2009), although there has been notable variation in findings (Fransson et al. 2007; Lin et al. 2008; Liu et al. 2008).

Utilizing standardized acquisition techniques, we obtained longitudinal fcMRI data from a cohort of preterm infants aged 26 weeks postmenstrual age (PMA) through term equivalent PMA. Infants were excluded from analysis if found to have significant abnormalities on conventional magnetic resonance imaging (MRI) studies. Employing seed-based correlation analysis, we identified resting state networks involving the sensorimotor, posterior cingulate, anterior cingulate, occipital, medial prefrontal, lateral prefrontal, and temporal cortices in addition to the thalamus and cerebellum, including networks not previously reported in preterm infants. In applying this neuroimaging technique to the study of preterm infants, we were able to identify the earliest forms of cerebral functional connectivity and characterize their development. In addition, by comparing fcMRI data collected from preterm infants at term equivalent PMA with those of healthy term-born infants, we identified disruption in the formation of thalamocortical connections believed to be critical for cortical organization (Kostovic and Jovanov-Milosevic 2006). Finally, investigation in term control infants identified connections between areas commonly cited as composing the default mode network, a collection of regions of increasing interest within the field of neuroscience (Fair et al. 2008).

Methods

Participants

Resting state fcMRI data sets were collected from preterm and term control infants recruited from the well-baby nursery and Neonatal Intensive Care Unit (NICU) at St Louis Children's Hospital as part of an ongoing study examining cerebral abnormalities associated with neurodevelopmental impairment in prematurely born children. Initial image acquisitions were performed within the first 2 weeks of life (as early as 26 weeks PMA). Based on clinical status and gestational age at

time of delivery, serial data sets for each infant were collected approximately every 4–5 weeks (30–31, 34–35, and 38–40 weeks PMA). Data from 10 term control infants (4 males) were also collected within 2–3 days of birth. Anatomical magnetic resonance images were reviewed by a neuroradiologist (J.S.S.) and pediatric neurologists (C.D.S. and T.E.I.). A total of 8 infants were excluded due to evidence of prominent neuropathology on anatomical scans, including 4 infants with high-grade (grade III/IV) intraventricular hemorrhage, 1 infant with multicystic periventricular leukomalacia, and 3 infants with cerebellar hemorrhage occupying greater than 20% of the total cerebellar volume. Within a subset of the remaining infants, a variable extent of intraventricular hemorrhage and white matter changes were noted, including 20 infants with low-grade (grade I/II) intraventricular hemorrhage, 15 infants with punctate T1 white matter hyperintensities less than 2 mm in size, 6 infants with microhemorrhagic lesions occupying less than 5% of the total cerebellar volume, and 19 infants with diffuse excessive high signal intensity on term equivalent PMA imaging study. There were no cerebral lesions in deep or cortical gray matter on conventional imaging in any subject. These criteria were selected in order to provide a study population in which the effects of common forms of neuropathology found in preterm infants were minimized.

A total of 90 data sets were collected from a total of 53 preterm infants. Longitudinal data sets were available for 28 infants, with data at the final 3 acquisition times available on 5 subjects. Due to decreased number of opportunities to study infants at the earliest age categories, the tenuous clinical status of very preterm infants, and movement artifact, fcMRI data were not available for any infant at each of the 4 acquisition times. Information regarding mean age at birth and time of scan for infants in each gestational age category is included in Table 1. Demographic information pertaining to sex, ethnicity, and mode of delivery for the infants is also provided. Data regarding individual subjects studied at specific acquisition points are also included (Supplementary Tables 1 and 2).

Data Acquisition

Images were collected on a Siemens Magnetom Trio 3T scanner utilizing an infant head coil produced by Advanced Imaging Research, Inc. Structural images were collected with an axial magnetization-prepared rapid gradient-echo (MP-RAGE) T1-weighted sequence (time repetition/echo time [TR/TE] 1550/3.05 ms and voxel size 1 mm^3) and a turbo spin-echo T2-weighted sequence (TR/TE 8950/161 ms, voxel size 1 mm^3, and echo train length 15). Functional images were collected utilizing a gradient-echo echo planar image sequence sensitized to $T2^*$ BOLD signal changes (TR/TE 2910/28 ms, voxel size 2.4 mm^3, flip angle 90°, field of view 151 mm, matrix size 64 × 64, and bandwidth 1662 Hz). Whole-brain coverage was obtained with 44 contiguous slices. A total of 200 frames were collected over 10 min. Total scan time for acquisition of all sequences was approximately 50 min. Identical collection techniques were applied for each infant.

Infants were studied during natural sleep or while resting quietly in the scanner without use of sedating medications. Subjects were prepared and transported to the scanner using institutional neonatal MRI guidelines (Mathur et al. 2008). Noise protection during scans was provided through use of neonatal earmuffs produced by Natus Medical, Inc. Arterial oxygen saturation and heart rate were continuously measured throughout image acquisition. An NICU staff member was present in the scanner room throughout each acquisition. Parental informed consent was obtained for each subject prior to participation in the study. Washington University School of Medicine's Human Studies Committee guidelines were followed for all aspects of the study.

fcMRI Analysis

Functional Data Preprocessing

All data underwent standard preprocessing to exclude signal change present due to nonneuronal causes. Slice-dependent time shifts were compensated and systematic odd–even slice intensity differences caused by interleaved acquisition were corrected. Images were intensity scaled to a whole-brain mode of 1000, excluding the first frame of each run (Ojemann et al. 1997). Movement analysis was performed using rigid body correction to account for head motion within and across runs. T2-weighted images were aligned with a gestational age–specific target to account for differences in cerebral volume across gestational age categories (Supplementary Figs 1 and 2). Affine transform to register the fcMRI first frame with the corrected T2-weighted image was then calculated. Data were realigned to the representative adult template used at the Washington University Neuroimaging Laboratory. This target is based on MP-RAGE T1-weighted data from 12 normal individuals and conforms to the Talairach atlas (Talairach and Tournoux 1988) as defined by spatial normalization procedure (Lancaster et al. 1995). fcMRI data were then converted to atlas space and resampled to 3-mm isotropic voxels. Comparability of functional data obtained from pediatric and adult subjects in common stereotactic space has been previously validated (Burgund et al. 2002; Kang et al. 2003).

Head motion generally was intermittent and did not preclude fcMRI analyses in most infants. Novel software tools were applied to identify frames containing significant motion via computation of signal change (evaluated by backward differences) averaged over the whole brain (developed by A.Z.S.; Supplementary Fig. 3). The most affected frames were excluded from further analysis (average number of frames removed per acquisition 44.2, range 0–114). A minimum of 4 min of utilizable BOLD data was required for inclusion in the present results. A total of 4 data sets were removed due to excessive motion artifact during BOLD acquisition. A total of 6 data sets were removed due to motion artifact during conventional imaging. These quality assurance measures, in combination with nuisance variable (time series from white matter and cerebrospinal fluid regions of interest) regression during fcMRI preprocessing, minimized the impact of spurious variance attributable to any cause, including subject motion.

A temporal band-pass filter for frequencies less than 0.08 Hz was applied. Linear regression analysis was performed utilizing 1) whole-brain signal averaged over a fixed region in atlas space, 2) 6 parameters obtained by rigid body analysis of head motion, 3) 10–12 white matter regions of interest (located in superior frontal, inferior frontal, superior parietal, occipital, and temporal lobes), and 4) 6–9 cerebrospinal fluid regions of interest (located in third ventricle, fourth ventricle, interpeduncular cistern, occipital horn of lateral ventricle, anterior horn of lateral ventricle, and superior extra-axial space) to remove sources of spurious variance. White matter and cerebrospinal fluid regions of interest were identified from the coregistered T2-weighted images utilizing a novel Matlab (MathWorks, Inc.) segmentation algorithm that differentiates gray matter, white matter, and cerebrospinal fluid regions with high resolution based on characteristic

Table 1
Image acquisition and demographic information for preterm infants categorized by PMA

PMA	Number of infants	Mean gestational age at birth (weeks)	Range (weeks)	Mean gestational age at scan (weeks)	Range (weeks)	Male, *n* (%)	Caucasian, *n* (%)	Vaginal delivery, *n* (%)
Less than 30 weeks	10	26.4	23.3–28.3	27.9	26.1–29.0	7 (70)	3 (30)	3 (30)
30 weeks	16	27.7	23.3–30.0	30.9	29.7–32.9	7 (44)	8 (50)	7 (44)
34 weeks	36	28.2	25.6–34.0	34.2	32.7–35.9	20 (53)	20 (53)	14 (39)
38 weeks	28	27.9	25.0–34.0	38.2	35.7–41.6	14 (50)	16 (57)	7 (25)
Term control	10							

patterns of signal intensity (developed by J.E.H.). Segmented white matter and cerebrospinal fluid regions were partitioned, followed by extraction and combination of time series for individual regions of interest. The nuisance regressor time series was then parsed through a singular value decomposition procedure to ensure that the regression linear system was algebraically well conditioned (maximum condition number = 100). Following regression analysis, data were spatially smoothed utilizing a 6-mm full-width at half-maximum Gaussian blur.

Correlation Analysis

The BOLD time series for multiple seed regions was cross-correlated with all other voxels in the brain, generating correlation maps identifying regions with functional connection to the region of interest. Seed regions were 6-mm spheres centered on regions of interest selected by a neuroradiologist (J.S.S.) based on prior study (Fox et al. 2005; Damoiseaux et al. 2006; Fair, Dosenbach, et al. 2007; Fransson et al. 2007; Fair et al. 2008). A total of 15 locations were examined in each hemisphere, including the thalamus; cerebellum; and sensorimotor, posterior cingulate, anterior cingulate, occipital, prefrontal, parietal, and temporal cortices (Fig. 1). Correlation coefficients were then converted to a normal distribution by Fisher's z transformation (Jenkins and Watts 1968), generating $z(r)$ correlation maps. These maps demonstrated the phenomenology of fcMRI activation across gestational age categories independent of group size (fixed-effects analysis). Results were displayed utilizing a $z(r)$ threshold of 0.3.

Statistical Analysis

Correlation maps were initially compared qualitatively across gestational age categories, with central tendencies in correlation strength between anatomical regions of interest and gestational age noted. In order to quantify identified differences and determine statistical significance, direct comparisons were performed between maps of interest utilizing one-tailed t-tests (assuming unequal variance) with subsequent conversion of t statistic values to equiprobable Z scores (random-effects analysis). Results were displayed utilizing a Z score threshold of 1.65 (corresponding to $P < 0.05$). In addition, utilizing the correlation maps generated for preterm infants, scatter plots were created illustrating the relationship between Fisher z-transformed correlation coefficient values for regions of interest (i.e., between homotopic counterparts) and PMA at time of image acquisition. Linear

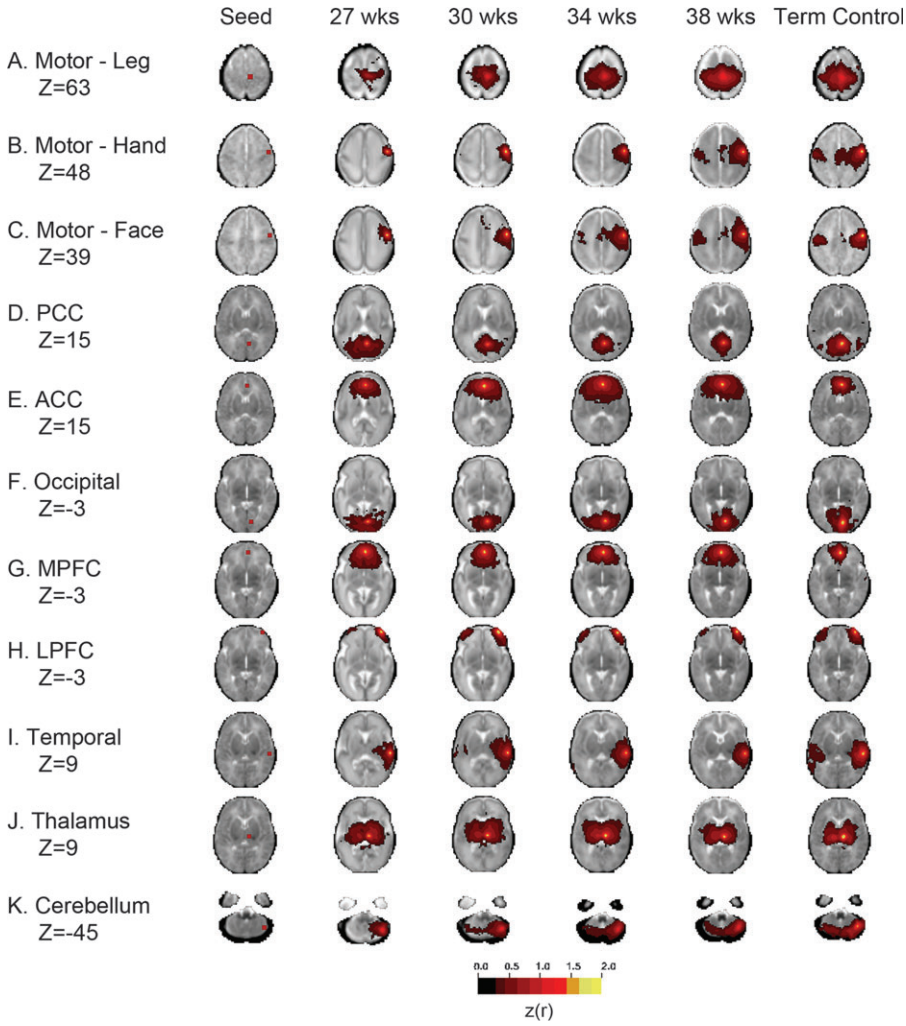

Figure 1. Longitudinal neural network development in preterm infants. Average fcMRI correlation maps corresponding to varied seed locations. The images are organized in columns corresponding to PMA at time of imaging. The illustrated quantity is the group mean Fisher z-transformed correlation coefficient (threshold value = 0.3) overlaid on the gestational age–specific atlas (Supplementary Figs 1 and 2). Each row shows the axial slice at the level of the seed region. Networks in preterm infants demonstrated limited intrahemispheric connectivity. Note age-dependent network maturation. Included are networks identified utilizing seeds located in the (*A*) motor cortex—leg ($Z = 63$), (*B*) motor cortex—hand ($Z = 48$), (*C*) motor cortex—face ($Z = 39$), (*D*) posterior cingulate cortex (PCC) ($Z = 15$), (*E*) anterior cingulate cortex (ACC) ($Z = 15$), (*F*) occipital cortex ($Z = -3$), (*G*) medial prefrontal cortex (MPFC) ($Z = -3$), (*H*) lateral prefrontal cortex (LPFC) ($Z = -3$), (*I*) temporal cortex ($Z = 9$), (*J*) thalamus ($Z = 9$), and (*K*) cerebellum ($Z = -45$). The right side of the image corresponds to the right side of the brain. The number of subjects contributing to each PMA group is 27 weeks, $n = 10$; 30 weeks, $n = 16$; 34 weeks, $n = 36$; 38 weeks, $n = 28$; and term control infants, $n = 10$ (see also Table 1 and Supplementary Table 1).

regression was subsequently performed to model the relationship between these 2 variables with generation of correlation coefficients and measures of significance. Of note, while independent activation in each hemisphere is manifest when utilizing midline seed locations, the effect of seed region and/or local activation extension into the contralateral hemisphere affecting correlation values in a contralateral region of interest following spatial smoothing cannot be definitively quantified (Supplementary Fig. 4).

Results

Neural Networks in Preterm Infants

Multiple networks demonstrating temporally correlated BOLD signal were identified utilizing seed correlation analysis (SCA) to analyze resting state fcMRI data collected from preterm and term control infants. These neural networks were identified utilizing seeds located in the sensorimotor (leg: Fig. 1*A*, hand: Fig. 1*B*, and face: Fig. 1*C*; Supplementary Figs 5 and 6), posterior cingulate (Fig. 1*D*), anterior cingulate (Fig. 1*E*), occipital (Fig. 1*F*), medial prefrontal (Fig. 1*G*), lateral prefrontal (Fig. 1*H*), and temporal (Fig. 1*I*) cortices, as well as thalamus (Fig. 1*J*) and cerebellum (Fig. 1*K*). Each network was identified as early as 26 weeks PMA and was detectable at each of the image acquisition time points (less than 30, 30–31, 34–35, and 38–40 weeks PMA). In general, networks identified later in development (greater PMA) consisted of localized interhemispheric connections between homotopic counterparts centered on regions of interest, with limited connection with other intrahemispheric locations. The sensorimotor areas were an exception, as connections to the ipsilateral supplementary motor areas were also detected. Investigation of the correlation maps demonstrated an age-dependent model of resting state network maturation with characteristic patterns of development as outlined below:

Connection Length Increases During Development—Neural Networks Identified Using Seed Locations at Greater Anatomical Distance from Their Homotopic Counterpart Established Interhemispheric Connections Later in Development

Networks identified utilizing medial seed locations demonstrated significant interhemispheric connectivity early in development, with connections between homotopic counterparts evident as early as 26 weeks PMA. In contrast, networks generated using lateral seed locations, regions at greater distance from their homotopic counterpart, initially demonstrated intensification of local connection strength, followed by emergence of bilateral connections later in development. In some cases, these correlations were not identified even at 38 weeks PMA. This difference is evident when contrasting the correlation maps generated using seeds located in the anterior cingulate, sensorimotor, and temporal cortices. As illustrated in Figure 1*E*, prominent interhemispheric connections were identified in a midline location such as the anterior cingulate cortex at 26 weeks PMA. In contrast, the network identified by placing a seed in the face region of the sensorimotor cortex (Fig. 1*C*), an area located laterally, did not demonstrate significant interhemispheric connection until much later in development. For this region, early correlations were unilateral, limited to connections centered on the region of interest. With advancing PMA, local associations intensified and expanded, with development of interhemispheric connections evident only between 34 and 38 weeks PMA. Finally, using a seed placed in the temporal cortex (Fig. 1*I*), the region furthest from its homotopic counterpart, interhemispheric connections were not identifiable in preterm infants even at 38 weeks PMA.

These patterns are also demonstrated when comparing the graphs generated by plotting measures of correlation between homotopic counterparts versus PMA for the same 3 regions. The right and left anterior cingulate cortices demonstrate significant interhemispheric connectivity from the earliest acquisition point, with limited variability (r = 0.058, P = 0.586) (Fig. 2*A*). This is contrasted with connections between the right and left face region of the sensorimotor cortex, which demonstrate a statistically significant increase in interhemispheric connectivity with advancing gestational age (r = 0.349, P = 0.001) (Fig. 2*B*). Finally, correlation between the right and left temporal cortex in preterm infants is limited throughout early development, with no significant change even at later acquisition times (r = 0.032, P = 0.766) (Fig. 2*C*).

Networks Identified Using Midline Seed Locations Were Initially Characterized by Regionally Widespread Interhemispheric Connectivity That Becomes More Localized with Development

In correlation maps generated from infants in the earliest gestational age categories, resting state networks were typically larger than those present at later PMA, initially incorporating wide areas of supplementary cortex and subcortical structures in addition to primary cortex. With maturation, these networks became more focused, with connections identified at later PMA being restricted to primary cortical regions. This is illustrated by the correlation maps generated utilizing an occipital cortex seed (Fig. 1*F*). Early forms of the network encompassed large areas of the primary and supplementary visual cortices with extension deep into surrounding subcortical regions. Examination of the networks generated later in development using an identical seed location demonstrated progression toward a more localized and defined network. By term equivalent PMA, the network was mainly limited to the primary visual cortex, decreasing in size nearly 10% from early forms (Supplementary Fig. 7). Similar patterns were observed for seeds in the posterior cingulate and medial prefrontal cortices as well as thalamus.

Neural Networks in Preterm Infants at Term Equivalent Age (38–40 Weeks PMA) Differed from Those Identified in Term Control Infants

Comparison of the networks generated for term control infants and preterm infants at term equivalent PMA, all of whom were assessed as having minimal cerebral injury, consistently demonstrated lower correlation and more limited distribution, including decreased long-range functional connectivity, in term equivalent infants. Examination of the correlation maps generated for these populations using a right thalamic seed illustrates this point (Fig. 3*A*). In correlations identified with a seed in this region, localized and interhemispheric connections in term control infants were more robust, with increased numbers of voxels in each hemisphere demonstrating stronger correlation. In addition, functional connections between the thalamus and sensorimotor cortex, brainstem, and cerebellar vermis were prominent in the term control infants. In contrast, for preterm infants at term equivalent PMA, significant correlations in the same region were more

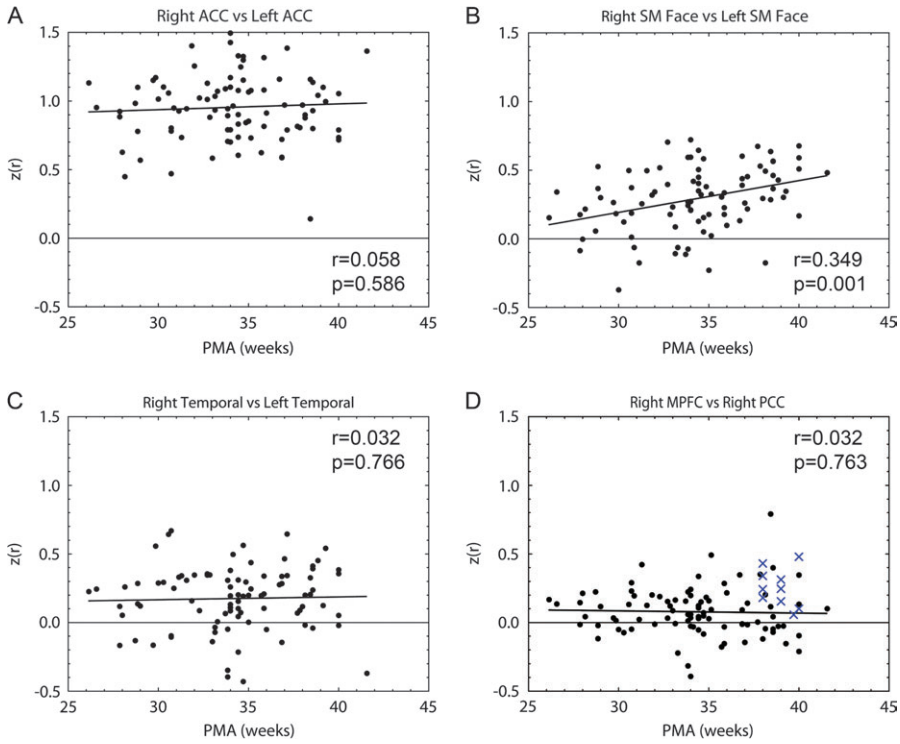

Figure 2. Functional connections demonstrate characteristic patterns of maturation based on location. Scatter plots demonstrating relationship between correlation values for regions of interest and PMA. Linear regression performed on result with correlation coefficient and measure of significance included. (*A*) Right and left anterior cingulate cortex (ACC) demonstrates significant interhemispheric connectivity between homotopic counterparts from earliest acquisition point with limited variability with advancing gestational age. Image is representative of those produced using medial seed locations. (*B*) Right and left sensorimotor (SM) cortex demonstrates statistically significant increase in interhemispheric connectivity between homotopic counterparts with advancing gestational age. Image is representative of those produced using lateral seed locations. (*C*) Right and left temporal cortex demonstrates limited interhemispheric connectivity between homotopic counterparts throughout early development. (*D*) Right medial prefrontal cortex (MPFC) and right posterior cingulate cortex (PCC) demonstrate limited connectivity between regions of interest in preterm infants (solid black circles), including those at term equivalent PMA. A subset of term control infants (blue Xs) demonstrate increased connectivity between these regions.

restricted, with limited connections identifiable between the thalamus and other areas involved in motor function. Direct comparison of these results by one-tailed *t*-test (random-effects analysis) confirms the statistical significance of these differences (Fig. 3*B*). This trend was apparent for each seed location, with more prominent differences observed with more lateral seed locations. Inclusion of only infants with limited to no white matter injury and no evidence of gray matter injury on conventional MRI in this analysis minimizes the role of neuropathology in this effect.

Longitudinal Analysis

To confirm results obtained utilizing all suitable preterm data sets, analysis employing identical techniques was performed with inclusion of data from the 5 infants for whom image sets at each of the final 3 acquisition points were available. Results obtained from this investigation were consistent with those previously described. Resting state networks involving each region of interest were again identified, with connections evident as early as 26 weeks PMA. Functional connections demonstrated an age-dependent pattern of development, with increasing correlation values and organization with advancing PMA. Varied rates of development of interhemispheric functional connectivity were evident depending on seed location. This result ensures that correlation maps obtained in the larger group analysis were not biased by inclusion of specific infant populations (i.e., infants born at later PMA). Representative examples of neural networks identified in this analysis are provided in Figure 4.

Default Mode Network

Additional analyses were performed to investigate functional connections between the regions most commonly cited as comprising the default mode network, including the medial prefrontal, posterior cingulate, parietal, and lateral temporal cortices, as well as the hippocampus (Fox et al. 2005). Utilizing a seed placed in the medial prefrontal cortex, associations between this region and the posterior cingulate cortex were identified qualitatively in term control infants. Connections between these and other regions comprising the default mode network were not evident using alternative seed locations in this population. Examples of the mean $z(r)$ maps illustrating these putative default mode network connections created using individual results from each term control infant are provided in Figure 5. Further quantitative analysis demonstrated that these results reflect emerging anterior–posterior connectivity in approximately half of the term infants, with a number of subjects within the group continuing to show limited connection strength between these regions. This is demonstrated on the graph generated by plotting measures of correlation between the medial prefrontal and posterior cingulate cortices versus PMA (blue Xs on Fig. 2*D*). The difference in results obtained utilizing qualitative and quantitative techniques underscores the importance of employing

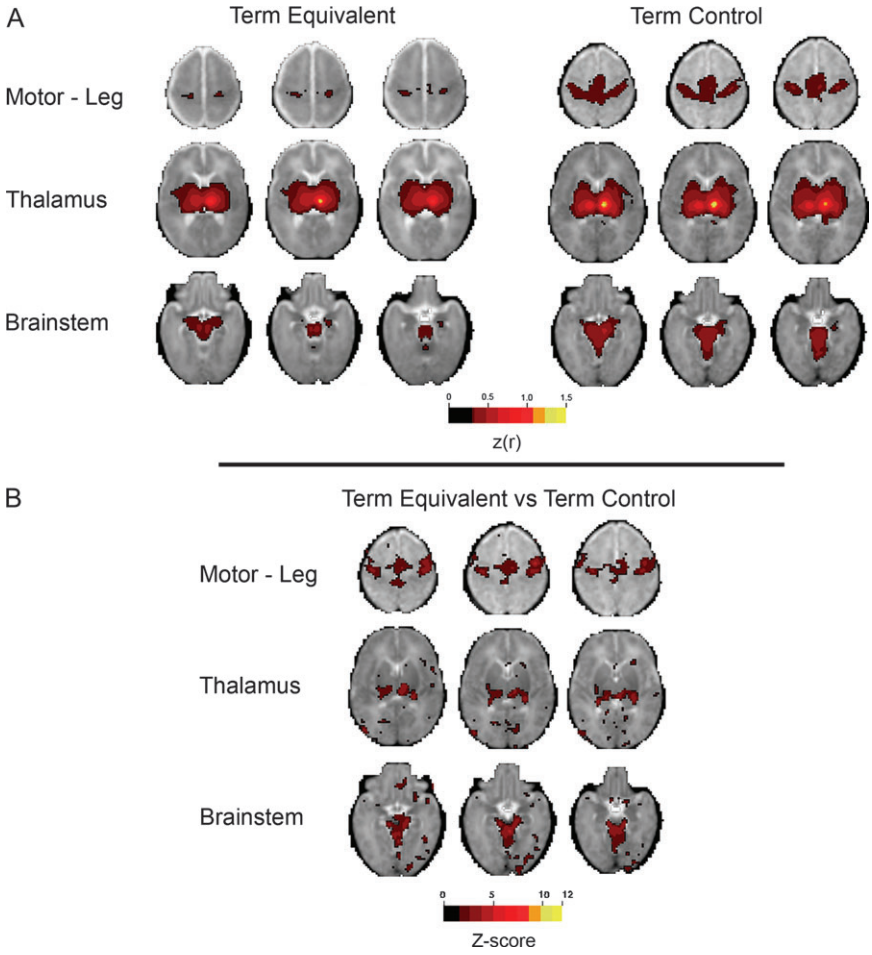

Figure 3. Significant differences in functional connectivity between term equivalent and term control infants using seed region located in the thalamus. (*A*) Average fcMRI correlation maps generated using a right thalamic seed demonstrating qualitative differences in functional connections between preterm infants at term equivalent PMA ($n = 28$) and term control infants ($n = 10$). Included are sensorimotor cortex—leg ($Z = 54/51/48$), thalamic ($Z = 12/9/6$), and brainstem ($Z = -15/-18/-21$) regions. The correlation map generated for the term equivalent infants demonstrates limited functional connections superiorly to the sensorimotor cortex and inferiorly to the brainstem and cerebellum in comparison with those identified for term control infants. $z(r)$ threshold 0.3 used. (*B*) These patterns are confirmed through direct comparison between these populations via voxel-wise *t*-test with subsequent conversion of *t* statistic values to equiprobable *Z* scores (random-effects analysis). Connections between the thalamus and sensorimotor cortex and brainstem and cerebellum are significantly stronger in term control infants. *Z* score threshold 1.65 (corresponding to $P < 0.05$) used. The right side of the image corresponds to the right side of the brain.

advanced tools in this type of analysis. Investigation of preterm infants in each of the gestational age categories using identical seed locations failed to identify connections between regions of the mature default mode network, including in preterm infants at term equivalent PMA. This is also illustrated in Figure 2*D* (black circles), which demonstrates limited correlation between the medial prefrontal and posterior cingulate cortices in preterm infants with advancing PMA ($r = 0.032$, $P = 0.763$).

Discussion

Through the study of very preterm infants, we have identified the earliest forms of cerebral functional connectivity and characterized resting state network maturation during the neonatal period. The networks located in the occipital, sensorimotor, temporal, posterior cingulate, and anterior cingulate cortices are consistent with those previously described in preterm infants (Fransson et al. 2007; Doria et al. 2008). Neural networks recognized using regions of interest in the medial and lateral prefrontal cortices and cerebellum have not been reported. As detailed above, these networks primarily consist of correlations between homotopic counterparts, with strong interhemispheric and limited intrahemispheric connectivity. This pattern differs from the neural networks described in adults, which are characterized by highly integrated interhemispheric and intrahemispheric connections between disparate regions (Fox et al. 2005; Damoiseaux et al. 2006; Dosenbach et al. 2007; Fair, Dosenbach, et al. 2007). Identified networks are more consistent with results obtained from young children (Fair et al. 2008; Lin et al. 2008; Thomason et al. 2008; Fransson et al. 2009; Kelly et al. 2009) and are presumed to represent immature forms of functional connections recognized in older populations.

The patterns of resting state network maturation described in this study are consistent with those of prior investigations in pediatric populations, with increasing strength, complexity, and regional variability detected across all periods of development (Fair, Dosenbach, et al. 2007; Fair, Schlaggar, et al. 2007; Thomason et al. 2008; Kelly et al. 2009). Lin et al. (2008) demonstrated a gradual increase in connection strength and

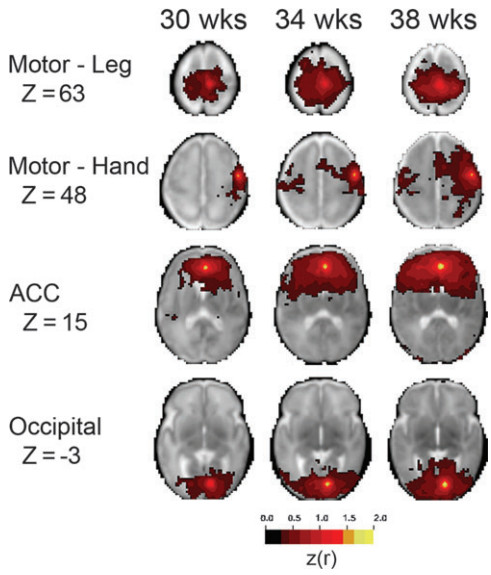

Figure 4. Results for infants with complete longitudinal data sets are consistent with those obtained for larger group analysis. Average fcMRI correlation maps generated using sensorimotor cortex—leg ($Z = 63$), sensorimotor cortex—hand ($Z = 48$), anterior cingulate cortex (ACC) ($Z = 15$), and occipital cortex ($Z = -3$) seed locations demonstrating longitudinal neural network development in 5 subjects studied at final 3 acquisition times. Results are similar to those from larger group analysis, demonstrating a comparable age-dependent pattern of development with increasing strength and organization with advancing gestational age. This demonstrates that correlation maps obtained in the larger group analysis were not biased by inclusion of specific infant populations. $z(r)$ threshold 0.3 used. The right side of the image corresponds to the right side of the brain.

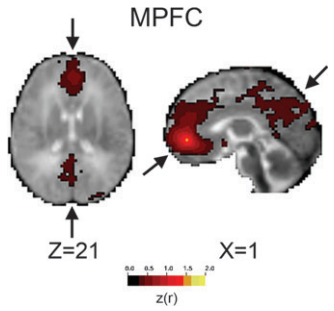

Figure 5. Default mode network precursors identified in term infants. Average fcMRI maps demonstrating putative default mode network precursors, including connections between the medial prefrontal and posterior cingulate cortices (arrows), identified in term control infants ($n = 10$) utilizing right medial prefrontal cortex (MPFC) seed location ($Z = 21$, $X = 1$). Further quantitative analysis demonstrates that these images likely reflect prominent anterior–posterior connectivity in a subset of these infants, with a number of infants within the group continuing to show limited connection strength between these regions. Comparable findings were not identified in preterm infants, including those at term equivalent PMA. $z(r)$ threshold 0.3 used. The right side of the image corresponds to the right side of the brain.

network size in the sensorimotor and occipital cortices between birth and 2 years of age, with variability in the rates of development between regions. This is similar to the increase in localized connection strength with maturation identified in our subjects. We also noted variability in the rate of connection development between regions. From childhood to adulthood, Kelly et al. (2009) noted a pattern of diffuse bilateral correlation that gradually became more defined in the anterior cingulate cortex. Variability based on seed location was also noted in this study. This is consistent with the pattern we found with medial seed locations. Finally, a series of publications have focused on the default mode network and other task control networks from childhood through early adulthood. Cohen et al. (2008), Fair, Dosenbach, et al. (2007), and Fair et al. (2008) described a process of resting state network maturation defined by "integration" (development of increased long-range functional connections) and "segregation" (decrease in short-range functional connections) between childhood and adulthood. Kelly et al. (2009) noted a similar phenomenon in their analysis, with increasing long-range correlation identified in older populations. In our study group, connections between widely separated homotopic counterparts (i.e., long-range connections) were identifiable only in older infants, while those between more midline locations (i.e., short-range connections) were identifiable early in development. N.B., this usage of "long-range" and "short-range" connections in the context of resting state networks should not be confused with similar application in the context of anatomy as clarified immediately below.

Development of Functional Connections

Anatomical and functional connectivity are interrelated but not identical (Vincent et al. 2007; Damoiseaux and Greicius 2009). We assume that functional connectivity strongly depends on anatomical connectivity, but the details of this relationship remain to be elucidated. It should be noted that all functional connectivity relates to what is termed long-range anatomical connections as distinguished from short-range (i.e., intracolumnar) connections. In our usage, the term "activity" refers to BOLD fluctuations. The available physiologic data indicate that BOLD fluctuations are neuronally driven and are more tightly coupled to dendritic activity than propagated action potentials (Logothetis 2002; Shmuel and Leopold 2008). Spontaneous, synchronous low-frequency (<0.1 Hz) fluctuations are the basis of resting state networks (Fox and Raichle 2007). The physiologic functions of resting state networks currently are not known.

Anatomical Connectivity Development

The development of functional connections is dependent on the establishment of cortical pathways and myelination of white matter. At birth, preterm infants possess a nearly adult number of poorly connected neurons (Lagercrantz and Changeux 2009). Thalamocortical connectivity and transient subplate synaptogenesis develop early in gestation, becoming increasingly prominent with advancing PMA (Kostovic and Rakic 1990). This is followed by the establishment of callosal and long-range cortical connections and regression of the temporary subplate from as early as 33 weeks PMA (Kostovic and Jovanov-Milosevic 2006). During this period, the elements critical to development of neural networks undergo gradual reformation, influenced by the ongoing production and subsequent elimination of transient exuberant projections and maturation of local neuronal activity (Innocenti and Price 2005). These evolving connections guide synaptogenesis and synaptic pruning and play an important role in the developmental patterns of cortical architecture (Chugani 1998) and electrical activity (Kostovic and Jovanov-Milosevic 2006). This process is influenced by both endogenous and sensory-driven activity, with environmental stimuli affecting synapse size, type, and distribution (Huttenlocher 1979; Bourgeois et al. 1989). Myelination also begins early in development and continues in

a hierarchical manner through early adulthood, with prominent changes during the period investigated in this study. Myelinated fibers enable efficient processing and the transfer of information between distinct anatomical regions, contributing significantly to the development and sustainability of functional connections (Fair, Dosenbach, et al. 2007; Cohen et al. 2008; Fair et al. 2008; Kelly et al. 2009). Neuroanatomical organization is further modulated via interaction with functional connections, with spontaneous synchronized neuronal activity impacting establishment of anatomical connections (Shatz 1996).

Spontaneous and Evoked Neuronal Activity

As noted previously, neural network development is also strongly influenced by spontaneous and evoked neuronal activity (Dosenbach et al. 2007; Fair, Dosenbach, et al. 2007; Kelly et al. 2009). Honey et al. (2007) demonstrated that spontaneous neuronal firing develops complex spatial and temporal patterns of activity independent of external input and change in neuroanatomical organization. This represents a process of "integration through synchronization" that is believed to play an integral role in early neural network development (Fair, Dosenbach, et al. 2007; Fair et al. 2008). Networks are also shaped by patterns of regional coactivation that occur in response to external stimuli, reflecting Hebbian strengthening of functional association based on experience (Dosenbach et al. 2007; Fair, Dosenbach, et al. 2007; Pinsk and Kastner 2007; Fair et al. 2008).

Complementary Investigational Techniques

Functional neurodevelopment has been explored in preterm infants using wide-ranging techniques, including assessment of stimulus-driven responses (functional magnetic resonance imaging), microstructural architecture (diffusion tensor imaging [DTI]), and electrical activity (electroencephalography [EEG]). Within each of these modalities, the spatial and temporal patterns of development are comparable with the results obtained in this study:

Functional Magnetic Resonance Imaging

Varied stimulus types have been shown to elicit stimulus-related cerebral activation in term-born infants as well as preterm infants at term equivalent PMA. Heep et al. (2009) demonstrated bilateral sensorimotor cortex activation with a passive unilateral motor task in 5 preterm infants at term equivalent PMA. Erberich et al. (2006) also used a passive unilateral motor task in a cohort of 24 infants that included preterm infants at term equivalent PMA to show a similar activation pattern. Finally, Born et al. (2000) established age-dependent patterns of bilateral response to visual stimuli in the occipital cortex in preterm infants at term equivalent PMA. The bilateral activation in infants (as compared with unilateral activation in adults) is consistent with our finding of larger areas of connectivity early in development. It is not known if this is the result of bilateral thalamic projections and/or transcallosal connections.

Diffusion Tensor Imaging

DTI has been utilized to study the microstructural architecture of the maturing brain. Recent investigation has demonstrated a process of gradual cerebral development, with variability between white and gray matter (Neil et al. 2002; Partridge et al. 2004). Characterization of functionally specific neuronal pathways via tractography has also demonstrated significant differences in the rate and pattern of development (Neil et al. 2002; Huppi and Dubois 2006). Changes within these networks are most pronounced during the period from 26 to 36 weeks PMA (Huppi and Dubois 2006), a period of development included in the present fcMRI study.

Electroencephalography

EEG in preterm infants has been well described, with early recordings characterized by intermittent bursts of electrical activity that become more continuous with advancing age. A hallmark of these studies is the presence of spontaneous activity transients (SATs) composed of brief, high-amplitude low-frequency signal (Vanhatalo and Kaila 2006). SATs have been identified as early as 24 weeks PMA and are initially localized to specific cortical regions with asynchronous activity (Niedermeyer and Lopes da Silva 2005). By 30–31 weeks PMA, SATs begin to demonstrate synchrony between hemispheres, and by 34–35 weeks PMA, temporal correlation becomes progressively more precise and consistent. During this period, interhemispheric synchronization is highest between homologous areas, and the rate of development varies significantly by region (Vanhatalo and Kaila 2006). At term age, recorded electrical activity is more synchronous, and SATs gradually disappear.

Results from each of these modalities suggest a common model of regionally variable age-dependent cerebral development based on structural and functional interhemispheric associations between homotopic counterparts. Prominent changes were noted with each technique during the developmental period investigated in this study. This consistent pattern suggests that these methods provide complementary approaches to the assessment of neurodevelopment and can be used in combination with functional connectivity to provide a more complete understanding of the interrelationship between structure and function.

Term versus Preterm Infants

This study demonstrated statistically significant differences in resting state network size and configuration for preterm infants without significant cerebral injury at term equivalent PMA when compared with healthy term-born control infants. In particular, the networks are less mature and/or abnormally formed in preterm infants, specifically with regard to thalamocortical connections. This is consistent with findings obtained using other MRI modalities and is presumed consequent to a combination of structural and environmental factors. Characteristic patterns of structural abnormality are recognizable in preterm infants by term equivalent PMA using high-resolution anatomical and DTI images, with cortical, deep nuclear gray, and white matter structures predominantly affected (Huppi et al. 1998; Inder et al. 2005; Anjari et al. 2007). These differences, including those involving thalamocortical connections, have been correlated with aberrant cognitive and motor performance in investigations of former preterm infants (Peterson et al. 2000; Nosarti et al. 2004; Woodward et al. 2006; Counsell et al. 2007). A limited number of studies have established the functional effects of these abnormalities as early as term equivalent PMA (Bassi et al. 2008).

A number of factors may play a role in the aberrant development of functional networks in preterm infants. The first may be injury to both white and gray matter. Injury to white matter disrupts connections directly, whereas injury to gray matter may alter the target of these connections. We note that infants with prominent injury (i.e., cystic periventricular leukomalacia, high-grade intraventricular hemorrhage, large cerebellar hemorrhage) detected by conventional MRI were excluded from this study, limiting the explanatory power of these factors in the present findings. In addition, the sensory experiences of preterm infants cared for in an intensive care unit are undoubtedly different from those of healthy term-born control infants. It is known that sensory deprivation during early childhood shapes resting state networks imaged during adulthood (Yu et al. 2008), but the effects of abnormal sensory experience on network development in premature infants are not yet understood. Even so, it is reasonable to suggest that abnormal neuronal interactions may, at least in part, underlie the significant disparity between term and preterm infants at term equivalent PMA. While it is suspected that these disparities represent early hallmarks of functional deficits in preterm infants, additional investigation is necessary to correlate these differences with structural abnormalities and long-term neurodevelopmental outcome.

Default Mode Network

Various default mode network precursors have been described in infants and children (Fransson et al. 2007, 2009; Doria et al. 2008; Fair et al. 2008; Thomason et al. 2008). Doria et al. (2008) and Fransson et al. (2007) both describe immature forms of this network in preterm infants, with Doria reporting associations between anterior and posterior regions and Fransson citing a "proto–default mode network" with posterior predominance. These networks do not include all of the regions classically considered to comprise the mature default mode network, which incorporates the medial prefrontal, posterior cingulate, parietal, and lateral temporal cortices, as well as the hippocampus. This underscores the difficulty in determining "true precursors" of this network (Gao et al. 2009). Our work did not demonstrate a network encompassing these areas in preterm infants, including premature infants at term equivalent PMA, with functional connections in these subjects again appearing less mature than those in term control infants. However, connections between these regions were identified in approximately half of the term control infants, suggesting the possible emergence of network precursors during this period. Further exploration of the pattern and rate of development of the default mode network in each of these populations is necessary.

Technical Considerations

Several technical issues must be considered when evaluating results obtained from this and other studies investigating functional connectivity in neonates.

Acquisition Parameters

fcMRI acquisition parameters can have significant impact on image quality and analysis results. In recently published investigations of functional connectivity, there have been important differences in spatial resolution and pulse sequence timing. For example, slice thickness has varied from 2.4 to 5 mm (Beckmann et al. 2005; Fox et al. 2005; Fransson et al. 2007; Liu et al. 2008; Long et al. 2008; Thomason et al. 2008), and TE has varied from 40 to 60 ms on 1.5T scanners and 25 to 30 ms on 3T scanners (Beckmann et al. 2005; Fox et al. 2005; Fransson et al. 2007; Liu et al. 2008; Long et al. 2008; Thomason et al. 2008). In this study, we used a slice thickness of 2.4 mm with isotropic voxels and a TE of 28 ms. In addition, methods by which appropriate acquisition parameters were identified have also varied significantly. Fransson et al. (2007) validated the parameters used in their study of infants by testing identical parameters in a single adult subject and reproducing 10 described resting state networks. Liu et al. (2008) selected image sequences based on the amount of audible noise produced during acquisition. The parameters used in this study were selected to provide the highest possible spatial resolution on our clinical scanners. To date, there has been no systematic study of optimal acquisition parameters for fcMRI data in neonates.

Level of Arousal

The effect of level of arousal on neural networks identified utilizing fcMRI remains incompletely understood, though the effects of sleep and anesthesia have been investigated (Vincent et al. 2007; Greicius et al. 2008; Horovitz et al. 2008, 2009; Larson-Prior LJ et al. 2009). Prior studies of functional connectivity in neonates have included results obtained from infants studied both with (Fransson et al. 2007; Doria et al. 2008) and without (Lin et al. 2008; Liu et al. 2008; Fransson et al. 2009; Gao et al. 2009) light sedation. In those performed without sedation, subjects are studied during natural sleep or while resting quietly, as in our study. Recent investigation in adult populations has suggested that resting state networks, including those located in the regions of interest examined in this study, are identifiable regardless of level of consciousness, though correlation strength may be modulated (Greicius et al. 2008; Horovitz et al. 2009). The effects of these factors on neural networks identified in this population require further investigation.

Analysis Technique

Multiple statistical analysis techniques are currently applied to identify spatial patterns of spontaneous BOLD activity (Fox and Raichle 2007). We employed SCA to identify neural networks. SCA is based on calculation of temporal correlation between a single region and all other regions of the brain. It requires a priori assumption of regions of interest and is not designed to study multiple systems simultaneously. This approach has been validated in adult and pediatric subjects (Fox et al. 2005; Fair, Dosenbach, et al. 2007; Fair et al. 2008; Lin et al. 2008). Additional studies have reported successful use of independent component analysis (ICA) to identify functional connections, including in neonates (Beckmann et al. 2005; Damoiseaux et al. 2006; Fransson et al. 2007, 2009). ICA utilizes statistical calculation to decompose data sets into separate components based on signal intensity time course of spatial maps. It is dependent on the number of components the analysis produces and requires a priori assumption for system selection (Fox and Raichle 2007). Recent literature has suggested that similar results are generated using both techniques (Beckmann et al. 2005; Long et al. 2008; Thomason et al. 2008), but this has not been validated in neonates.

Regions of Interest

Seed locations utilized in the current study were selected based on previous published investigations of functional

connectivity (Fox et al. 2005; Damoiseaux et al. 2006; Fair, Dosenbach, et al. 2007; Fransson et al. 2007; Fair et al. 2008). A limited number of regions were examined. It is likely that there are additional regions to be investigated in this population. Furthermore, small differences in seed location can have significant impact on the identified neural networks (Cohen et al. 2008). Systematic study utilizing increasing numbers and varied locations for regions of interest in preterm infants is necessary.

Movement

Despite efforts to limit subject movement during image acquisition, motion artifact was observed in multiple data sets. Novel software tools were developed and applied to identify and remove significantly affected volumes in order to minimize the impact of intermittent head motion on the present results (Supplementary Fig. 3). Ten data sets were completely excluded due to excessive motion at varied stages of acquisition. This number compares favorably with other studies in this population but can be improved. While these measures limited the ability to perform within-subject longitudinal analysis in specific instances, they are critical to minimizing the effects of motion artifact in measured results. Refinement of acquisition and analysis techniques may further minimize effects of motion in this type of analysis.

Conclusions

Defining the functional organization of the human brain during the neonatal period is an important step in understanding the mechanisms of normal and aberrant neurodevelopment. Through the longitudinal investigation of preterm infants using resting state fcMRI, we characterized the earliest forms of functional cerebral connections, established the presence of multiple neural networks, and detailed a regionally variable age-specific pattern of network maturation that parallels those reported in older children. These patterns reflect the complex interplay of structural and functional processes that occurs throughout early development and are consistent with results obtained in prior investigations of neurodevelopment during this critical period. This study demonstrates the viability of this imaging modality as an early developmental biomarker and lays the groundwork for future study of neurological disorders and neuroprotective interventions in this vulnerable population.

Funding

National Institutes of Health (grant numbers RO1 HD05709801 to T.E.I. and J.J.N., K23 HD053212 to J.S.S., and P30 NS048056) and the Doris Duke Foundation (grant number 3187-41956 to T.E.I.).

Notes

The authors would like to thank Bradley L. Schlaggar for analysis advice and helpful discussion and J. Lauren Lambeth for assistance with data analysis. The funders had no role in study design, data collection and analysis, decision to publish, or preparation of the manuscript. *Conflict of Interest*: None declared.

References

Anjari M, Srinivasan L, Allsop JM, Hajnal JV, Rutherford MA, Edwards AD, Counsell SJ. 2007. Diffusion tensor imaging with tract-based spatial statistics reveals local white matter abnormalities in preterm infants. Neuroimage. 35:1021–1027.

Bassi L, Ricci D, Volzone A, Allsop JM, Srinivasan L, Pai A, Ribes C, Ramenghi LA, Mercuri E, Mosca F, et al. 2008. Probabilistic diffusion tractography of the optic radiations and visual function in preterm infants at term equivalent age. Brain. 131:573–582.

Beckmann CF, DeLuca M, Devlin JT, Smith SM. 2005. Investigations into resting-state connectivity using independent component analysis. Philos Trans R Soc Lond B Biol Sci. 360:1001–1013.

Biswal B, Yetkin FZ, Haughton VM, Hyde JS. 1995. Functional connectivity in the motor cortex of resting human brain using echo-planar MRI. Magn Reson Med. 34:537–541.

Born AP, Miranda MJ, Rostrup E, Toft PB, Peitersen B, Larsson HB, Lou HC. 2000. Functional magnetic resonance imaging of the normal and abnormal visual system in early life. Neuropediatrics. 31:24–32.

Bourgeois JP, Jastreboff PJ, Rakic P. 1989. Synaptogenesis in visual cortex of normal and preterm monkeys: evidence for intrinsic regulation of synaptic overproduction. Proc Natl Acad Sci U S A. 86:4297–4301.

Burgund ED, Kang HC, Kelly JE, Buckner RL, Snyder AZ, Petersen SE, Schlaggar BL. 2002. The feasibility of a common stereotactic space for children and adults in fMRI studies of development. Neuroimage. 17:184–200.

Chugani HT. 1998. A critical period of brain development: studies of cerebral glucose utilization with PET. Prev Med. 27:184–188.

Cohen AL, Fair DA, Dosenbach NU, Miezin FM, Dierker D, Van Essen DC, Schlaggar BL, Petersen SE. 2008. Defining functional areas in individual human brains using resting functional connectivity MRI. Neuroimage. 41:45–57.

Counsell SJ, Dyet LE, Larkman DJ, Nunes RG, Boardman JP, Allsop JM, Fitzpatrick J, Srinivasan L, Cowan FM, Hajnal JV, et al. 2007. Thalamo-cortical connectivity in children born preterm mapped using probabilistic magnetic resonance tractography. Neuroimage. 34:896–904.

Damoiseaux JS, Greicius MD. 2009. Greater than the sum of its parts: a review of studies combining structural connectivity and resting-state functional connectivity. Brain Struct Funct. 213:525–533.

Damoiseaux JS, Rombouts SA, Barkhof F, Scheltens P, Stam CJ, Smith SM, Beckmann CF. 2006. Consistent resting-state networks across healthy subjects. Proc Natl Acad Sci U S A. 103:13848–13853.

Doria V, Beckmann CF, Rees G, Nunes RG, Merchant N, Counsell S, Edwards D. 2008. Spontaneous brain activity in infants from 33 weeks gestational age [abstract]. Washington (DC): Society for Neuroscience. Program No. 787.13/SS50.

Dosenbach NU, Fair DA, Miezin FM, Cohen AL, Wenger KK, Dosenbach RA, Fox MD, Snyder AZ, Vincent JL, Raichle ME, et al. 2007. Distinct brain networks for adaptive and stable task control in humans. Proc Natl Acad Sci U S A. 104:11073–11078.

Erberich SG, Panigrahy A, Friedlich P, Seri I, Nelson MD, Gilles F. 2006. Somatosensory lateralization in the newborn brain. Neuroimage. 29:155–161.

Fair DA, Cohen AL, Dosenbach NU, Church JA, Miezin FM, Barch DM, Raichle ME, Petersen SE, Schlaggar BL. 2008. The maturing architecture of the brain's default network. Proc Natl Acad Sci U S A. 105:4028–4032.

Fair DA, Dosenbach NU, Church JA, Cohen AL, Brahmbhatt S, Miezin FM, Barch DM, Raichle ME, Petersen SE, Schlaggar BL. 2007. Development of distinct control networks through segregation and integration. Proc Natl Acad Sci U S A. 104:13507–13512.

Fair DA, Schlaggar BL, Cohen AL, Miezin FM, Dosenbach NU, Wenger KK, Fox MD, Snyder AZ, Raichle ME, Petersen SE. 2007. A method for using blocked and event-related fMRI data to study "resting state" functional connectivity. Neuroimage. 35:396–405.

Fox MD, Raichle ME. 2007. Spontaneous fluctuations in brain activity observed with functional magnetic resonance imaging. Nat Rev Neurosci. 8:700–711.

Fox MD, Snyder AZ, Vincent JL, Corbetta M, Van Essen DC, Raichle ME. 2005. The human brain is intrinsically organized into dynamic, anticorrelated functional networks. Proc Natl Acad Sci U S A. 102:9673–9678.

Fransson P, Skiold B, Engstrom M, Hallberg B, Mosskin M, Aden U, Lagercrantz H, Blennow M. 2009. Spontaneous brain activity in the

newborn brain during natural sleep—an fMRI study in infants born at full term. Pediatr Res. 66:301–305.
Fransson P, Skiold B, Horsch S, Nordell A, Blennow M, Lagercrantz H, Aden U. 2007. Resting-state networks in the infant brain. Proc Natl Acad Sci U S A. 104:15531–15536.
Gao W, Zhu H, Giovanello KS, Smith JK, Shen D, Gilmore JH, Lin W. 2009. Evidence on the emergence of the brain's default network from 2-week-old to 2-year-old healthy pediatric subjects. Proc Natl Acad Sci U S A. 106:6790–6795.
Greicius MD, Kiviniemi V, Tervonen O, Vainionpää V, Alahuhta S, Reiss AL, Menon V. 2008. Persistent default-mode network connectivity during light sedation. Hum Brain Mapp. 29:839–847.
Heep A, Scheef L, Jankowski J, Born M, Zimmermann N, Sival D, Bos A, Gieseke J, Bartmann P, Schild H, et al. 2009. Functional magnetic resonance imaging of the sensorimotor system in preterm infants. Pediatrics. 123:294–300.
Honey CJ, Kotter R, Breakspear M, Sporns O. 2007. Network structure of cerebral cortex shapes functional connectivity on multiple time scales. Proc Natl Acad Sci U S A. 104:10240–10245.
Horovitz SG, Braun AR, Carr WS, Picchioni D, Balkin TJ, Fukunaga M, Duyn JH. 2009. Decoupling of the brain's default mode network during deep sleep. Proc Natl Acad Sci U S A. 106:11376–11381.
Horovitz SG, Fukunaga M, de Zwart JA, van Gelderen P, Fulton SC, Balkin TJ, Duyn JH. 2008. Low frequency BOLD fluctuations during resting wakefulness and light sleep: a simultaneous EEG-fMRI study. Hum Brain Mapp. 29:671–682.
Huppi PS, Dubois J. 2006. Diffusion tensor imaging of brain development. Semin Fetal Neonatal Med. 11:489–497.
Huppi PS, Warfield S, Kikinis R, Barnes PD, Zientara GP, Jolesz FA, Tsuji MK, Volpe JJ. 1998. Quantitative magnetic resonance imaging of brain development in premature and mature newborns. Ann Neurol. 43:224–235.
Huttenlocher PR. 1979. Synaptic density in human frontal cortex—developmental changes and effects of aging. Brain Res. 163:195–205.
Inder TE, Warfield SK, Wang H, Huppi PS, Volpe JJ. 2005. Abnormal cerebral structure is present at term in premature infants. Pediatrics. 115:286–294.
Innocenti GM, Price DJ. 2005. Exuberance in the development of cortical networks. Nat Rev Neurosci. 6:955–965.
Jenkins GM, Watts DG. 1968. Spectral analysis and its applications. San Francisco (CA): Holden-Day.
Kang CK, Burgund ED, Lugar HM, Petersen SE, Schlaggar BL. 2003. Comparison of functional activation foci in children and adults using a common stereotactic space. Neuroimage. 19:16–28.
Kelly AM, Di Martino A, Uddin LQ, Shehzad Z, Gee DG, Reiss PT, Margulies DS, Castellanos FX, Milham MP. 2009. Development of anterior cingulate functional connectivity from late childhood to early adulthood. Cereb Cortex. 19:640–657.
Kostovic I, Jovanov-Milosevic N. 2006. The development of cerebral connections during the first 20-45 weeks' gestation. Semin Fetal Neonatal Med. 11:415–422.
Kostovic I, Rakic P. 1990. Developmental history of the transient subplate zone in the visual and somatosensory cortex of the macaque monkey and human brain. J Comp Neurol. 297:441–470.
Lagercrantz H, Changeux JP. 2009. The emergence of human consciousness: from fetal to neonatal life. Pediatr Res. 65: 255–260.
Lancaster JL, Glass TG, Lankipalli BR, Downs H, Mayberg H, Fox PT. 1995. A modality-independent approach to spatial normalization of tomographic images of the human brain. Hum Brain Mapp. 3:209–223.
Larson-Prior LJ, Zempel JM, Nolan TS, Prior FW, Snyder AZ, Raichle ME. 2009. Cortical network functional connectivity in the descent to sleep. Proc Natl Acad Sci U S A. 106:4489–4494.
Lin W, Zhu Q, Gao W, Chen Y, Toh CH, Styner M, Gerig G, Smith JK, Biswal B, Gilmore JH. 2008. Functional connectivity MR imaging reveals cortical functional connectivity in the developing brain. AJNR Am J Neuroradiol. 29:1883–1889.
Liu WC, Flax JF, Guise KG, Sukul V, Benasich AA. 2008. Functional connectivity of the sensorimotor area in naturally sleeping infants. Brain Res. 1223:42–49.
Logothetis NK. 2002. The neural basis of the blood-oxygen-level-dependent functional magnetic resonance imaging signal. Philos Trans R Soc Lond B Biol Sci. 357:1003–1037.
Long XY, Zuo XN, Kiviniemi V, Yang Y, Zou QH, Zhu CZ, Jiang TZ, Yang H, Gong QY, Wang L, et al. 2008. Default mode network as revealed with multiple methods for resting-state functional MRI analysis. J Neurosci Methods. 171:349–355.
Lowe MJ, Mock BJ, Sorenson JA. 1998. Functional connectivity in single and multislice echoplanar imaging using resting-state fluctuations. Neuroimage. 7:119–132.
Mathur AM, Neil JJ, McKinstry RC, Inder TE. 2008. Transport, monitoring, and successful brain MR imaging in unsedated neonates. Pediatr Radiol. 38:260–264.
Neil J, Miller J, Mukherjee P, Huppi PS. 2002. Diffusion tensor imaging of normal and injured developing human brain—a technical review. NMR Biomed. 15:543–552.
Niedermeyer E, Lopes da Silva FH. 2005. Electroencephalography: basic principles, clinical applications, and related fields. Philadelphia: Lippincott Williams & Wilkins.
Nosarti C, Rushe TM, Woodruff PW, Stewart AL, Rifkin L, Murray RM. 2004. Corpus callosum size and very preterm birth: relationship to neuropsychological outcome. Brain. 127:2080–2089.
Ojemann JG, Akbudak E, Snyder AZ, McKinstry RC, Raichle ME, Conturo TE. 1997. Anatomic localization and quantitative analysis of gradient refocused echo-planar fMRI susceptibility artifacts. Neuroimage. 6:156–167.
Partridge SC, Mukherjee P, Henry RG, Miller SP, Berman JI, Jin H, Lu Y, Glenn OA, Ferriero DM, Barkovich AJ, et al. 2004. Diffusion tensor imaging: serial quantitation of white matter tract maturity in premature newborns. Neuroimage. 22:1302–1314.
Penn AA, Shatz CJ. 1999. Brain waves and brain wiring: the role of endogenous and sensory-driven neural activity in development. Pediatr Res. 45:447–458.
Peterson BS, Vohr B, Staib LH, Cannistraci CJ, Dolberg A, Schneider KC, Katz KH, Westerveld M, Sparrow S, Anderson AW, et al. 2000. Regional brain volume abnormalities and long-term cognitive outcome in preterm infants. JAMA. 284:1939–1947.
Pinsk MA, Kastner S. 2007. Neuroscience: unconscious networking. Nature. 447:46–47.
Raichle ME, MacLeod AM, Snyder AZ, Powers WJ, Gusnard DA, Shulman GL. 2001. A default mode of brain function. Proc Natl Acad Sci U S A. 98:676–682.
Rowland DJ, Garbow JR, Laforest R, Snyder AZ. 2005. Registration of [^{18}F]FDG microPET and small-animal MRI. Nucl Med Biol. 32:567–572.
Shatz CJ. 1996. Emergence of order in visual system development. Proc Natl Acad Sci U S A. 93:602–608.
Shmuel A, Leopold DA. 2008. Neuronal correlates of spontaneous fluctuations in fMRI signals in monkey visual cortex: implications for functional connectivity at rest. Hum Brain Mapp. 29:751–761.
Talairach J, Tournoux P. 1988. Co-planar stereotaxic atlas of the human brain: 3-D proportional system: an approach to cerebral imaging. New York: Thieme Medical.
Thomason ME, Chang CE, Glover GH, Gabrieli JD, Greicius MD, Gotlib IH. 2008. Default-mode function and task-induced deactivation have overlapping brain substrates in children. Neuroimage. 41:1493–1503.
Vanhatalo S, Kaila K. 2006. Development of neonatal EEG activity: from phenomenology to physiology. Semin Fetal Neonatal Med. 11:471–478.
Vincent JL, Patel GH, Fox MD, Snyder AZ, Baker JT, Van Essen DC, Zempel JM, Snyder LH, Corbetta M, Raichle ME. 2007. Intrinsic functional architecture in the anaesthetized monkey brain. Nature. 447:83–86.
Woodward LJ, Anderson PJ, Austin NC, Howard K, Inder TE. 2006. Neonatal MRI to predict neurodevelopmental outcomes in preterm infants. N Engl J Med. 355:685–694.
Yu C, Liu Y, Li J, Zhou Y, Wang K, Tian L, Qin W, Jiang T, Li K. 2008. Altered functional connectivity of primary visual cortex in early blindness. Hum Brain Mapp. 29:533–543.